Hindawi Publishing Corporation
Journal of Applied Mathematics
Volume 2014, Article ID 907152, 7 pages
http://dx.doi.org/10.1155/2014/907152

Research Article

The Magnetohydrodynamic Boundary Layer Flow of a Nanofluid past a Stretching/Shrinking Sheet with Slip Boundary Conditions

Syahira Mansur[1] and Anuar Ishak[2]

[1] *Department of Mathematics and Statistics, Faculty of Science, Technology and Human Development, Universiti Tun Hussein Onn Malaysia, Batu Pahat, 86400 Parit Raja, Johor, Malaysia*
[2] *Centre for Modelling & Data Analysis, School of Mathematical Sciences, Faculty of Science and Technology, Universiti Kebangsaan Malaysia, 43600 Bangi, Selangor, Malaysia*

Correspondence should be addressed to Anuar Ishak; anuarishak@yahoo.com

Received 4 December 2013; Accepted 14 February 2014; Published 17 March 2014

Academic Editor: Junjie Wei

The magnetohydrodynamic (MHD) boundary layer flow of a nanofluid past a stretching/shrinking sheet with velocity, thermal, and solutal slip boundary conditions is studied. Numerical solutions to the governing equations were obtained using a shooting method. The skin friction coefficient and the local Sherwood number increase as the stretching/shrinking parameter increases. However, the local Nusselt number decreases with increasing the stretching/shrinking parameter. The range of the stretching/shrinking parameter for which the solution exists increases as the velocity slip parameter and the magnetic parameter increase. For the shrinking sheet, the skin friction coefficient increases as the velocity slip parameter and the magnetic parameter increase. For the stretching sheet, it decreases when the velocity slip parameter and the magnetic parameter increase. The local Nusselt number diminishes as the thermal slip parameter increases while the local Sherwood number decreases with increasing the solutal slip parameter. The local Nusselt number is lower for higher values of Lewis number, Brownian motion parameter, and thermophoresis parameter.

1. Introduction

The boundary layer flow over a stretching sheet is significant in applications such as extrusion, wire drawing, metal spinning, and hot rolling [1]. Wang [2, 3], Mandal and Mukhopadhyay [4], P. S. Gupta and A. S. Gupta [5], Andersson [6], Ishak et al. [7], and Makinde and Aziz [8] are among various names whose papers on stretching sheet were published. However, to complement the study of flow over a stretching sheet, Miklavčič and Wang [9] then began the study of flow over a shrinking sheet in which they observed that the vorticity is not confined within a boundary layer and a steady flow cannot exist without exerting adequate suction at the boundary. As the studies of shrinking sheet garnered considerable attention, these findings prove to be crucial to these researches. In response to Miklavčič and Wang [9], numerous studies on these problems have been conducted by researchers, namely, Wang [10], Fang et al. [11], Bachok et al. [12], Bhattacharyya et al. [13], Zaimi et al. [14], and Roşca and Pop [15], among others.

However, most studies were done in the absence of magnetic field. Ishak et al. [16] studied the magnetohydrodynamic (MHD) stagnation point flow towards a stretching sheet while Merkin and Kumaran [17] studied the unsteady MHD boundary layer flow on a shrinking sheet.

Motivated by the above-mentioned studies, this paper aims at studying the MHD boundary layer flow of a nanofluid over a stretching/shrinking sheet with slip conditions and suction effect at the boundary. The inclusion of nanoparticles enhances thermal conductivity as reported by Masuda et al. [18]. This study will use the model developed by Buongiorno [19] where we pay more attention to the Brownian motion and thermophoresis effects as previously done by Nield and Kuznetsov [20–22]. In addition, we employ the velocity

and thermal and solutal slip conditions because the recent findings that rarefied gas flows with slip boundary conditions are often encountered in the microscale devices and low-pressure situations (Kumaran and Pop [23]). The effects of slip conditions are very important in technological applications such as in the polishing of artificial heart valves and the internal cavities. For the shrinking case, the solution does not exist since vorticity could not be confined within the boundary layer. However, with an added suction effect to confine the vorticity, the solution may exist. The dependency of the local skin friction coefficient, Nusselt number, and Sherwood number on seven parameters, namely, the stretching/shrinking, velocity slip, thermal slip, concentration slip, magnetic, Brownian motion, and thermophoresis parameters, is the main focus of the present investigation. Numerical solutions are presented graphically and in tabular forms to show the effects of these parameters on the local Nusselt number and the local Sherwood number.

2. Mathematical Formulation

Consider a steady, two-dimensional boundary layer flow of a nanofluid over a permeable stretching/shrinking sheet. It is assumed that the stretching/shrinking velocity is in the form $U_w = ax$, where a is a positive constant and x is the coordinate measured along the stretching/shrinking surface. It is also assumed that the constant mass flux velocity is v_0 with $v_0 < 0$ for suction and $v_0 > 0$ for injection or withdrawal of the fluid. The nanofluid is confined to $y > 0$, where y is the coordinate measured normal to the stretching/shrinking surface. The flow is subjected to the transverse magnetic field of strength B_0, which is assumed to be applied in the positive y-direction. The induced magnetic field is also assumed to be small compared to the applied magnetic field; hence, it is neglected.

The governing equations for the steady conservation of mass, momentum, thermal energy, and nanoparticle volume fraction equations in the presence of magnetic field can be written as [19, 20, 22, 24]

$$\frac{\partial u}{\partial x} + \frac{\partial v}{\partial y} = 0, \tag{1}$$

$$u\frac{\partial u}{\partial x} + v\frac{\partial u}{\partial y} = -\frac{1}{\rho_f}\frac{\partial p}{\partial x} + \omega\left(\frac{\partial^2 u}{\partial x^2} + \frac{\partial^2 u}{\partial y^2}\right) - \frac{\lambda B_0^2}{\rho_f}u, \tag{2}$$

$$u\frac{\partial v}{\partial x} + v\frac{\partial v}{\partial y} = -\frac{1}{\rho_f}\frac{\partial p}{\partial y} + \omega\left(\frac{\partial^2 v}{\partial x^2} + \frac{\partial^2 v}{\partial y^2}\right) - \frac{\lambda B_0^2}{\rho_f}v, \tag{3}$$

$$u\frac{\partial T}{\partial x} + v\frac{\partial T}{\partial y} = \alpha\left(\frac{\partial^2 T}{\partial x^2} + \frac{\partial^2 T}{\partial y^2}\right) + \tau\left\{D_B\left(\frac{\partial \varphi}{\partial x}\frac{\partial T}{\partial x} + \frac{\partial \varphi}{\partial y}\frac{\partial T}{\partial y}\right) + \frac{D_T}{T_\infty}\left[\left(\frac{\partial T}{\partial x}\right)^2 + \left(\frac{\partial T}{\partial y}\right)^2\right]\right\}, \tag{4}$$

$$u\frac{\partial \varphi}{\partial x} + v\frac{\partial \varphi}{\partial y} = D_B\left(\frac{\partial^2 \varphi}{\partial x^2} + \frac{\partial^2 \varphi}{\partial y^2}\right) + \frac{D_T}{T_\infty}\left(\frac{\partial^2 T}{\partial x^2} + \frac{\partial^2 T}{\partial y^2}\right), \tag{5}$$

where u and v are the velocity components along the x- and y-axes respectively, p is the fluid pressure, T is the fluid temperature, α is the thermal diffusivity, ω is the kinematic viscosity, λ is the electrical conductivity, B_0 is the magnetic field, D_B is the Brownian diffusion coefficient, D_T is the thermophoresis diffusion coefficient, and φ is the nanoparticle volume fraction. Furthermore, $\tau = (\rho c)_p/(\rho c)_f$ is the ratio between the effective heat capacity of the fluid with ρ_f and ρ_p being the density of the fluid and the density of the particles, respectively, and c_f and c_p denote the specific heat of the fluid and the particle at constant pressure, respectively. The subscript ∞ represents the values at large values of y (outside the boundary layer). Details of the derivation of (4) and (5) are given in the papers by Buongiorno [19] and Nield and Kuznetsov [21].

Equations (1)–(5) are subjected to the following boundary conditions [24]:

$$v = v_0, \quad u = \sigma U_w + L\frac{\partial u}{\partial y}, \quad T = T_w + K_1\frac{\partial T}{\partial y}, \quad \varphi = \varphi_w + K_2\frac{\partial \varphi}{\partial y} \quad \text{at } y = 0, \tag{6}$$

$$u \longrightarrow 0, \quad v \longrightarrow 0, \quad T \longrightarrow T_\infty, \quad \varphi \longrightarrow \varphi_\infty \quad \text{as } y \longrightarrow \infty, \tag{7}$$

where σ is a constant with $\sigma > 0$ for stretching and $\sigma < 0$ for shrinking. The subscript w denotes the values at the solid surface. Furthermore, L, K_1, and K_2 are the velocity, thermal, and solutal slip factors, respectively and when $L = K_1 = K_2 = 0$, the no-slip condition is recovered. The governing equations (1)–(5) subjected to the boundary conditions (6) and (7) can be expressed in a simpler form by introducing the following transformation:

$$\psi = (U_w \omega x)^{1/2} f(\eta), \qquad \eta = \left(\frac{U_w}{\omega x}\right)^{1/2} y, \qquad \theta(\eta) = \frac{T - T_\infty}{T_f - T_\infty}, \qquad \beta(\eta) = \frac{\varphi - \varphi_\infty}{\varphi_w - \varphi_\infty}, \tag{8}$$

where η is the similarity variable and ψ is the stream function defined as $u = \partial\psi/\partial y$ and $v = -\partial\psi/\partial x$, which identically satisfy (1). By employing the boundary layer approximations and the similarity variables (8), (2)–(5) reduce to the following nonlinear ordinary differential equations:

$$f''' + ff'' - f'^2 - Mf' = 0, \tag{9}$$

$$\frac{1}{\mathrm{Pr}}\theta'' + f\theta' + \mathrm{Nb}\beta'\theta' + \mathrm{Nt}\theta'^2 = 0, \tag{10}$$

$$\beta'' + \frac{\mathrm{Nt}}{\mathrm{Nb}}\theta'' + \mathrm{Le}f\beta' = 0 \tag{11}$$

and the boundary conditions (6) and (7) become

$$f(0) = S, \qquad f'(0) = \sigma + Af''(0),$$
$$\theta(0) = 1 + B\theta'(0), \qquad \beta(0) = 1 + C\beta'(0), \tag{12}$$

$$f' = 0, \quad \theta = 0, \quad \beta = 0 \quad \text{as } \eta \longrightarrow \infty, \tag{13}$$

where primes denote differentiation with respect to η. Further, Pr is the Prandtl number, Nb is the Brownian motion parameter, Nt is the thermophoresis parameter, Le is the Lewis number, S is the mass flux parameter with $S > 0$ for suction and $S < 0$ for injection, M is the magnetic parameter, and A, B, and C are velocity, thermal, and solutal slip parameters respectively, which are defined as

$$\text{Pr} = \frac{\omega}{\alpha}, \qquad \text{Nb} = \frac{\tau D_B(\varphi_w - \varphi_\infty)}{\omega},$$
$$\text{Nt} = \frac{\tau D_T(T_w - T_\infty)}{\omega T_\infty}, \qquad \text{Le} = \frac{\omega}{D_B},$$
$$S = -\frac{v_0}{\sqrt{a\omega}}, \qquad M = \frac{\lambda B_0^2}{\rho_f a}, \qquad A = L\sqrt{\frac{a}{\omega}}, \tag{14}$$
$$B = K_1\sqrt{\frac{a}{\omega}}, \qquad C = K_2\sqrt{\frac{a}{\omega}};$$

when Nb = Nt = 0, the present problem reduces to a regular viscous fluid, and the nanoparticle volume fraction equation (11) becomes ill-posed and is of no physical significance.

The physical quantities of interest are the skin friction coefficient C_f, the local Nusselt number Nu_x, and the local Sherwood number Sh_x which are defined as [6]

$$C_f = -\frac{\tau_w}{\rho U_w^2}, \qquad \text{Nu}_x = \frac{xq_w}{k(T_f - T_\infty)},$$
$$\text{Sh}_x = \frac{xq_m}{D_B(\varphi_w - \varphi_\infty)}, \tag{15}$$

where τ_w, q_w, and q_m are the surface shear stress, the heat and mass fluxes, respectively, which are given by [25]

$$\tau_w = \mu\left(\frac{\partial u}{\partial y}\right)_{y=0}, \qquad q_w = -k\left(\frac{\partial T}{\partial y}\right)_{y=0},$$
$$q_m = -D_B\left(\frac{\partial \varphi}{\partial y}\right)_{y=0}. \tag{16}$$

Using the similarity variables (8), we obtain

$$C_f\text{Re}_x^{1/2} = -f''(0), \qquad \text{Nu}_x\text{Re}_x^{-1/2} = -\theta'(0),$$
$$\text{Sh}_x\text{Re}_x^{-1/2} = -\beta'(0), \tag{17}$$

where $\text{Re}_x = U_w x/\omega$ is the local Reynolds number.

3. Results and Discussions

The set of ordinary differential equations (9)–(11) subjected to boundary conditions (12) and (13) were solved numerically using a shooting method. In this method, the dual solutions are obtained by setting different initial guesses for the values of $f''(0)$, $-\theta'(0)$ and $-\beta'(0)$. The asymptotic boundary conditions (13) at $\eta = \infty$ are replaced by $\eta = 15$ which is sufficient for all the velocity, temperature, and concentration profiles to vanish asymptotically.

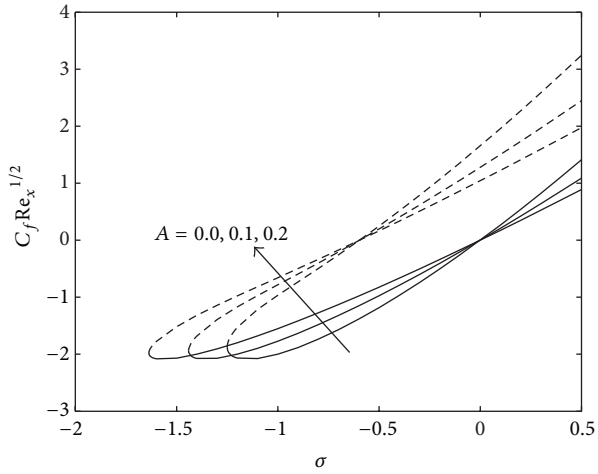

Figure 1: Variation of the skin friction coefficient with σ for different values of A when $S = 3$ and $M = 1$.

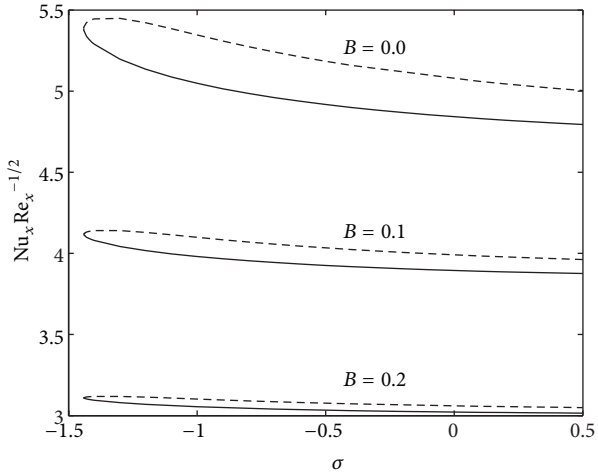

Figure 2: Variation of the local Nusselt number with σ for different values of B when $S = 3$, $M = 1$, Pr = 6.8, $A = C = 0.1$, Nt = Nb = 0.5, and Le = 2.

Figures 1–3 show the variations of the local skin friction coefficient $C_f\text{Re}_x^{1/2}$, the local Nusselt number $\text{Nu}_x\text{Re}_x^{-1/2}$ (representing the heat transfer rate at the surface), and the local Sherwood number $\text{Sh}_x\text{Re}_x^{-1/2}$ (representing the mass transfer rate at the surface) with σ for different values of the velocity slip parameter A, thermal slip parameter B, and solutal slip parameter C, respectively. As can be seen, there are more than one solution obtained for a fixed value of σ. When σ is equal to a certain value $\sigma = \sigma_c$ where $\sigma_c(< 0)$ is the critical value of σ, there is only one solution, and when $\sigma < \sigma_c$, there is no solution. Here, the computations have

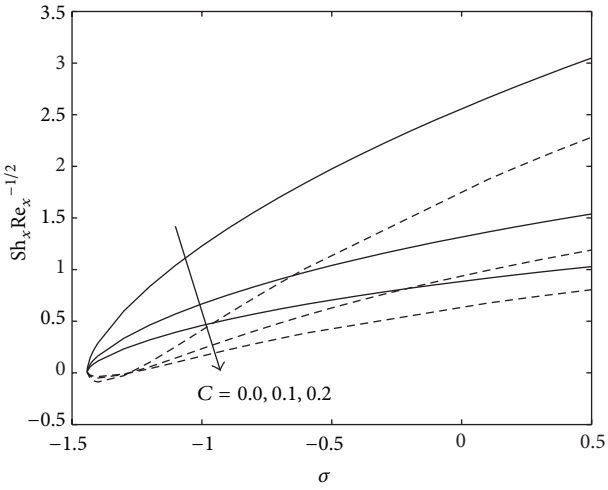

Figure 3: Variation of the local Sherwood number with σ for different values of C when $S = 3$, $M = 1$, Pr = 6.8, $A = B = 0.1$, Nt = Nb = 0.5, and Le = 2.

Table 1: Values of σ_c for several values of S and A.

S	A	σ_c
3	0.1	−1.4400
4		−2.6128
5		−3.3948
3	0.0	−1.2500
	0.2	−1.6368

been performed until the point where the solution does not converge. Based on our computations, the critical values σ_c are presented in Table 1. The range of σ for which the solution exists increases as A and S increase. For an increasing slip parameter at the boundary, the generation of vorticity for shrinking velocity is slightly reduced [13]. Therefore, with the imposed suction, that vorticity remains confined in the boundary layer region for larger shrinking velocity (i.e., $\sigma < 0$). Hence, the steady solution is possible for some large values of σ. Although only the first solution is stable and physically realizable [15, 26, 27], the second solution is of mathematical interest as the differential equations are concerned.

From Figures 1–3, the skin friction coefficient, the local Nusselt number, and the local Sherwood number change accordingly with the change of shrinking/stretching parameter σ, velocity slip A, thermal slip B, and solutal slip C. As σ increases, the skin friction coefficient and the local Sherwood number increase. On the other hand, the local Nusselt number decreases as σ increases. Furthermore, the change occurring in the local Nusselt number is very small as compared to the skin friction coefficient and the local Sherwood number.

Figure 1 portrays the skin friction coefficient for different values of A, the velocity slip parameter. The graph shows that the differences are uniform for all values of A and σ. It is interesting to see the different characteristics possessed by the shrinking and stretching sheets. We can see that for

Table 2: Variations of the skin friction coefficient $-f''(0)$, local Nusselt number $-\theta'(0)$, and local Sherwood number $-\beta'(0)$ for (a) stretching and (b) shrinking sheets at $A = 0.1$ for different values of S and M.

(a)

S	M	$-f''(0)$
3	0.1	1.180642
4		1.444545
5		1.676866
3	0.0	1.189619
	1.0	1.087972
	1.5	1.022694

(b)

S	M	$-f''(0)$
3	0.1	−2.105103
4		−2.743993
5		−3.261509
3	0.0	−2.131948
	1.0	−1.771988
	1.5	−0.956086

shrinking sheet ($\sigma < 0$), the skin friction coefficient increases with A. Yet, the opposite is true for the stretching sheet ($\sigma > 0$) where the skin friction coefficient decreases as A increases. This trait is again seen in Table 2 where we computed values of the skin friction coefficient with different values of S and M. For stretching sheet, the skin friction increases as S increases while the increment in M lowers the skin friction coefficient. On the other hand, for the shrinking sheet, the skin friction coefficient decreases as S increases and increases with increasing M. The changes occurring for a shrinking sheet is more pronounced than those of a stretching sheet. For example, this observation can be seen when M is increased, where the difference in the skin friction coefficient is approximately 10% for a stretching sheet and 35% for a shrinking sheet.

Figure 2 shows the variations of the local Nusselt number for different values of B. The surface heat transfer rate is consistently lower for higher thermal slip parameter B. This phenomenon agrees with the findings of Aman et al. [28]. The diminishing rate may be caused by the increase in thermal boundary layer thickness. Although the change in the local Nusselt number is uniform as B is increased, it is more pronounced than the change occurring in the skin friction coefficient and the local Sherwood number (Figure 3).

Through Figure 3, we can see the effect of the solutal slip parameter C on the local Sherwood number. As C increases, the local Sherwood number decreases consistently. It is worth to note that as we apply the solutal slip condition to a previously no-slip condition ($C = 0$), the values reduce abruptly where the change is approximately 50%. However as C increases from 0.1 to 0.2, the difference between the resulting surface mass transfer rates is lower where the difference is about 40%.

Table 3: Variations of the local Nusselt number $-\theta'(0)$ and local Sherwood number $-\beta'(0)$ at Le = 2, $M = 1$, $S = 3$, $A = B = C = 0.1$, Pr = 6.8, and $\sigma = -1$ for different values of Nt and Nb.

Nt = Nb	Le	$-\theta'(0)$	$-\beta'(0)$
0.1	2	6.236334	−0.328127
0.3		5.139931	0.355463
0.5		3.885173	1.139644
0.1	3	6.156869	1.350187
	5	6.099435	3.461077
	7	6.093712	4.736331

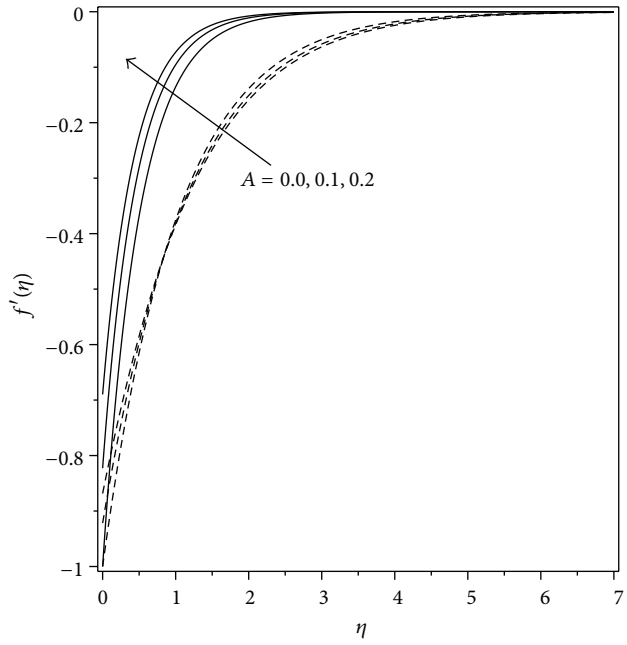

Figure 4: The velocity profiles for different values of A when $S = 3$, $M = 1$, and $\sigma = -1$.

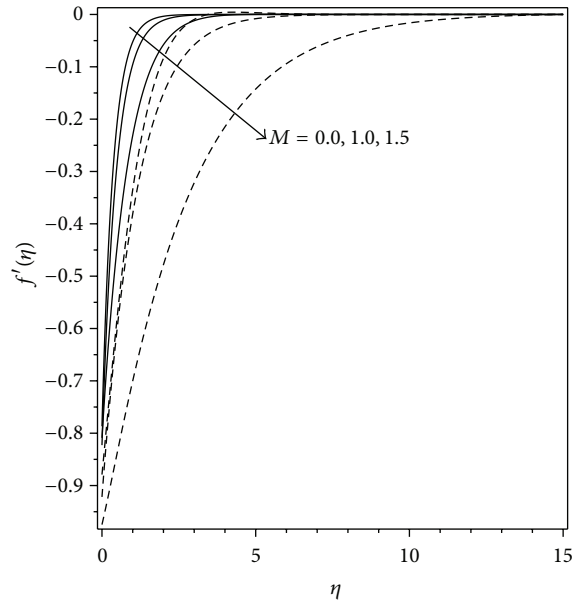

Figure 5: The velocity profiles for different values of M when $S = 3$, $A = 0.1$, and $\sigma = -1$.

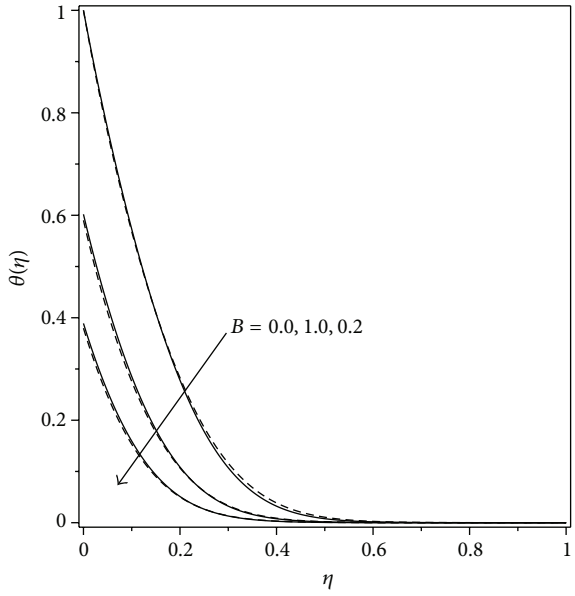

Figure 6: The temperature profiles for different values of B when $S = 3$, $M = 1$, Pr = 6.8, $A = C = 0.1$, Nt = Nb = 0.5, Le = 2, and $\sigma = -1$.

Table 3 presents the variations of the local Nusselt and Sherwood numbers as we manipulate both thermophoresis and Brownian motion parameters (Nt = Nb) and Lewis number Le. As Nt and Nb increase, the local Nusselt number decreases while the local Sherwood number increases. The negative values of the local Sherwood number imply that the surface is losing mass. The local Nusselt number also reacts negatively when Le is increased. However, the mass transfer rate at the surface increases with Le. Although not shown, the thermal boundary layer thickness increases while the concentration boundary layer thickness decreases as Le is increased which causes this effect.

The samples of velocity, temperature, and concentration profiles for shrinking sheet are included in Figures 4–8. These profiles satisfy the far field boundary condition (13) asymptotically, which support the numerical results obtained besides supporting the existence of dual solutions shown in Figures 1–3. Figures 4 and 5 show the velocity profiles for different values of A and M, respectively. As A is increased, the velocity also increases. However, as M increases, the velocity decreases due to the retarding effect resulted from the presence of transverse magnetic field [24]. Hence, as M increases, the retarding force increases and thus the velocity decreases.

Through Figures 6 and 7, we can see the effect of B and Nt = Nb on the temperature profiles. The temperature lowers as B is increased. However, it increases as both Nt and Nb increase due to the fact that Nt is directly proportional to the heat transfer coefficient associated with the fluid [24]. It is also observed that the boundary layer thickness decreases with

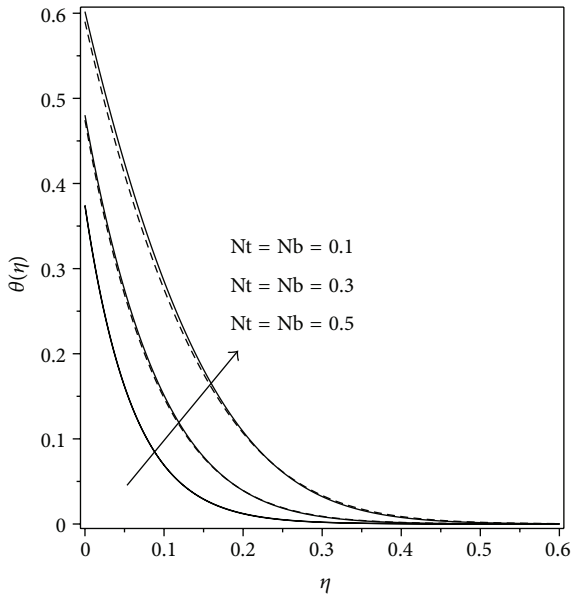

Figure 7: The temperature profiles for different values of Nt(= Nb) when $S = 3$, $M = 1$, Pr = 6.8, $A = B = C = 0.1$, Le = 2, and $\sigma = -1$.

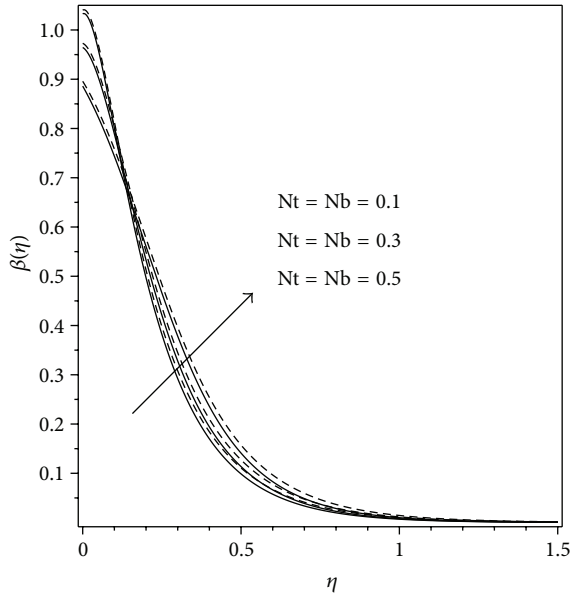

Figure 8: The concentration profiles for different values of Nt(= Nb) when $S = 3$, $M = 1$, Pr = 6.8, $A = B = C = 0.1$, Le = 2, and $\sigma = -1$.

increasing B. On the other hand, the boundary layer thickness increases as both Nt and Nb are increased. This may be the probable cause of the diminishing the local Nusselt number in Figure 2 and Table 3.

The concentration profiles for different values of Nt (= Nb) are shown in Figure 8. Due to the dependency of the concentration on the temperature field, we expect that a higher thermophoresis would allow a deeper penetration of the concentration [29]. As a result, we can see from Figure 8 that the concentration increases as we increase both Nt and Nb. In addition, we can also note that at the surface and its surrounding area, the concentration decreases with the increasing Nt and Nb.

4. Conclusions

The MHD boundary layer flow of a nanofluid past a stretching/shrinking sheet with hydrodynamic, thermal, and solutal slip boundary conditions was studied. Numerical solutions to the governing equations were obtained using a shooting method. A few observations have been made in this paper as follows.

(1) The range of the stretching/shrinking parameter for which the solution exists increases as velocity slip parameter A increases.

(2) For a shrinking sheet, the skin friction coefficient increases with the velocity slip parameter A and magnetic parameter M. For a stretching sheet, it decreases when the velocity slip parameter and magnetic parameter are increased. The changes occurring in shrinking sheet are more pronounced than those in the stretching sheet. As M increases, the difference in the skin friction coefficient is approximately 10% for a stretching sheet and 35% for a shrinking sheet.

(3) The local Nusselt number diminishes as thermal slip parameter B increases while the local Sherwood number decreases with increasing values of the solutal slip parameter C.

(4) Increasing the Lewis number and both thermophoresis parameter and Brownian motion parameter is to decrease the local Nusselt number and the local Sherwood number.

Conflict of Interests

The authors declare that there is no conflict of interests regarding the publication of this paper.

Acknowledgments

The financial supports received from the Ministry of Higher Education, Malaysia (Project code FRGS/1/2012/SG04/UKM/01/1) and the Universiti Kebangsaan Malaysia (Project code DIP-2012-31) are gratefully acknowledged.

References

[1] E. G. Fischer, *Extrusion of Plastics*, Wiley, New York, NY, USA, 1976.

[2] C. Y. Wang, "Flow due to a stretching boundary with partial slip—an exact solution of the Navier-Stokes equations," *Chemical Engineering Science*, vol. 57, no. 17, pp. 3745–3747, 2002.

[3] C. Y. Wang, "Analysis of viscous flow due to a stretching sheet with surface slip and suction," *Nonlinear Analysis: Real World Applications*, vol. 10, no. 1, pp. 375–380, 2009.

[4] I. C. Mandal and S. Mukhopadhyay, "Heat transfer analysis for fluid flow over an exponentially stretching porous sheet with surface heat flux in porous medium," *Ain Shams Engineering Journal*, vol. 4, no. 1, pp. 103–110, 2013.

[5] P. S. Gupta and A. S. Gupta, "Heat and mass transfer on a stretching sheet with suction or blowing," *The Canadian Journal of Chemical Engineering*, vol. 55, no. 6, pp. 744–746, 1977.

[6] H. I. Andersson, "Slip flow past a stretching surface," *Acta Mechanica*, vol. 158, no. 1-2, pp. 121–125, 2002.

[7] A. Ishak, R. Nazar, and I. Pop, "Heat transfer over an unsteady stretching permeable surface with prescribed wall temperature," *Nonlinear Analysis: Real World Applications*, vol. 10, no. 5, pp. 2909–2913, 2009.

[8] O. D. Makinde and A. Aziz, "Boundary layer flow of a nanofluid past a stretching sheet with a convective boundary condition," *International Journal of Thermal Sciences*, vol. 50, no. 7, pp. 1326–1332, 2011.

[9] M. Miklavčič and C. Y. Wang, "Viscous flow due to a shrinking sheet," *Quarterly of Applied Mathematics*, vol. 64, no. 2, pp. 283–290, 2006.

[10] C. Y. Wang, "Stagnation flow towards a shrinking sheet," *International Journal of Non-Linear Mechanics*, vol. 43, no. 5, pp. 377–382, 2008.

[11] T. Fang, S. Yao, J. Zhang, and A. Aziz, "Viscous flow over a shrinking sheet with a second order slip flow model," *Communications in Nonlinear Science and Numerical Simulation*, vol. 15, no. 7, pp. 1831–1842, 2010.

[12] N. Bachok, A. Ishak, and I. Pop, "Stagnation-point flow over a stretching/shrinking sheet in a nanofluid," *Nanoscale Research Letters*, vol. 6, no. 623, pp. 1–10, 2011.

[13] K. Bhattacharyya, S. Mukhopadhyay, and G. C. Layek, "Slip effects on boundary layer stagnation-point flow and heat transfer towards a shrinking sheet," *International Journal of Heat and Mass Transfer*, vol. 54, no. 1–3, pp. 308–313, 2011.

[14] K. Zaimi, A. Ishak, and I. Pop, "Boundary layer flow and heat transfer past a permeable shrinking sheet in a nanofluid with radiation effect," *Advances in Mechanical Engineering*, vol. 2012, Article ID 340354, 7 pages, 2012.

[15] A. V. Roşca and I. Pop, "Flow and heat transfer over a vertical permeable stretching/shrinking sheet with a second order slip," *International Journal of Heat and Mass Transfer*, vol. 60, pp. 355–364, 2013.

[16] A. Ishak, K. Jafar, R. Nazar, and I. Pop, "MHD stagnation point flow towards a stretching sheet," *Physica A: Statistical Mechanics and its Applications*, vol. 388, no. 17, pp. 3377–3383, 2009.

[17] J. H. Merkin and V. Kumaran, "The unsteady MHD boundary-layer flow on a shrinking sheet," *European Journal of Mechanics, B/Fluids*, vol. 29, no. 5, pp. 357–363, 2010.

[18] H. Masuda, A. Ebata, K. Teramae, and N. Hishinuma, "Alteration of thermal conductivity and viscosity of liquid by dispersing ultra-fine particles," *Japan Journal of Thermophysical Properties*, vol. 7, no. 4, pp. 227–233, 1993.

[19] J. Buongiorno, "Convective transport in nanofluids," *Journal of Heat Transfer*, vol. 128, no. 3, pp. 240–250, 2006.

[20] D. A. Nield and A. V. Kuznetsov, "The Cheng-Minkowycz problem for natural convective boundary-layer flow in a porous medium saturated by a nanofluid," *International Journal of Heat and Mass Transfer*, vol. 52, no. 25-26, pp. 5792–5795, 2009.

[21] D. A. Nield and A. V. Kuznetsov, "Thermal instability in a porous medium layer saturated by a nanofluid," *International Journal of Heat and Mass Transfer*, vol. 52, no. 25-26, pp. 5796–5801, 2009.

[22] D. A. Nield and A. V. Kuznetsov, "The Cheng-Minkowycz problem for the double-diffusive natural convective boundary layer flow in a porous medium saturated by a nanofluid," *International Journal of Heat and Mass Transfer*, vol. 54, no. 1–3, pp. 374–378, 2011.

[23] V. Kumaran and I. Pop, "Nearly parallel blasius flow with slip," *Communications in Nonlinear Science and Numerical Simulation*, vol. 16, no. 12, pp. 4619–4624, 2011.

[24] W. Ibrahim and B. Shankar, "MHD boundary layer flow and heat transfer of a nanofluid past a permeable stretching sheet with velocity, thermal and solutal slip boundary conditions," *Computers and Fluids*, vol. 75, pp. 1–10, 2013.

[25] N. Bachok, A. Ishak, and I. Pop, "Unsteady boundary-layer flow and heat transfer of a nanofluid over a permeable stretching/shrinking sheet," *International Journal of Heat and Mass Transfer*, vol. 55, no. 7-8, pp. 2102–2109, 2012.

[26] P. D. Weidman, D. G. Kubitschek, and A. M. J. Davis, "The effect of transpiration on self-similar boundary layer flow over moving surfaces," *International Journal of Engineering Science*, vol. 44, no. 11-12, pp. 730–737, 2006.

[27] A. Postelnicu and I. Pop, "Falkner-Skan boundary layer flow of a power-law fluid past a stretching wedge," *Applied Mathematics and Computation*, vol. 217, no. 9, pp. 4359–4368, 2011.

[28] F. Aman, A. Ishak, and I. Pop, "Mixed convection boundary layer flow near stagnation-point on vertical surface with slip," *Applied Mathematics and Mechanics*, vol. 32, no. 12, pp. 1599–1606, 2011.

[29] A. Rasekh, D. D. Ganji, and S. Tavakoli, "Numerical solutions for a nanofluid past over a stretching circular cylinder with non-uniform heat source," *Frontiers in Heat and Mass Transfer*, vol. 3, Article ID 043003, pp. 1–6, 2012.